ERF 2001 Paper No. 70

SMART STRUCTURE TECHNOLOGY & CONTROL OF BUFFET INDUCED HELICOPTER VIBRATIONS

S. Hanagud, X. Lu and R. Roglin

School of Aerospace Engineering
Georgia Tech, Atlanta, Georgia 30332-0150

ABSTRACT

Helicopters are susceptible to buffet induced vibrations of control surfaces. The control surface vibrations can result in vibrations in the cockpit because of the typical design of rotorcraft fuselage that includes the usual mass distribution, the inertia distribution and the locations of heavy components. In the past, many design modifications and passive vibration control techniques have been used to reduce the buffet induced vibrations in rotorcraft. In this paper, a method of designing an active structural control to minimize the amplitude of these buffet-induced oscillatory loads and the resulting responses is presented. The design of the active structural controller is based on the use of an offset piezoceramic stack actuator assembly and acceleration feedback control. A method of estimating the number of piezoceramic stacks and the associated design parameters of the actuator assembly, to control the buffet induced vibrations, is discussed.

INTRODUCTION

1. Stabilizer Buffeting

Many helicopters and rotorcraft are susceptible to the stabilizer buffet. The stabilizer buffet has been observed in rotorcraft like V-22 and RAH-66. The reasons for the stabilizer buffet have been attributed to high angle of attack operations and the aerodynamic shapes of the fuselage of these rotorcraft. Sometimes, the bluff aerodynamic shape of the rotorcraft results from the design to accommodate low observability requirements.

An important consequence of the stabilizer buffet is the buffet induced vibrations of the vertical stabilizer. Because of the typical design of the rotorcraft fuselage, the vibrations of the vertical stabilizer cause vibrations of the fuselage and the horizontal stabilizer when it is used in the design. In some rotorcraft, vibrations induced by the stabilizer buffet are further enhanced because of the unsymmetric design of the rotorcraft. For example, in some helicopters, stabilizer buffet induced vibrations are observed at angles of attack ranging from 4 to 20 degrees and at forward speeds in the range of 40 to 165 knots. Buffet induced vibrations at low angles of attack are attributed to the bluff aerodynamic shapes. The stabilizer buffet and the resulting vibrations are a problem in some currently operational rotorcraft[1].

Even though the stabilizer buffet induced vibrations significantly contribute to the overall vibrations of a helicopter or a rotorcraft, a significant amount of attention has been given only to the control of the higher harmonic vibrations that are observed at frequencies corresponding to integral multiples per revolution of the rotor. Other sources of rotorcraft vibrations that have received attention are the self-excitated vibrations due to flutter, ground resonance and vibrations transmitted by the engine and the transmission. Very little effort has been devoted to the reduction of buffet induced vibrations.

2. Buffet Induced Vibrations and Their Control

To date, the source and the mechanism of the stabilizer buffet are not well understood. However, the turbulence induced by the bluff aerodynamic shape and the vortices shed by the rotor/fuselage system are suspected to be the causes. A direct effect of these unsteady air loads is the vibration of the empennage. Then, because of the typical design of a rotorcraft fuselage (mass distribution, inertia distribution and the location of the heavy components), the induced empennage vibrations can cause the vibration of the cockpit and the horizontal stabilizer. The resulting effects of these buffet-induced vibrations can be of the same order as the other sources of vibration and include fatigue damage, a restriction on the maneuver capability and the fatigue of the pilot and the crew.

An aerodynamic solution is to use strakes to modify the flow and thus reduce the magnitude of buffet loads. This approach has serious adverse effects and can reduce the flight envelope. Several passive structural solutions are sought. This includes stiffening brackets, modifying the design of the

horizontal stabilizer, stiffening the aft stabilizer cone and stiffening the vertical stabilizer. Such passive structural modifications, in a fixed wing aircraft, have not been able to eliminate or even significantly reduce the buffet load induced vibrations and the resulting fatigue damage[6][22].

An active control option is to use smart or adaptive structures concept to attenuate the buffet-induced (unsteady air load induced) vibrations. In the proposed approach, the objective is not to oscillate an aerodynamic surface like a flap that can produce control loads to counter the air loads due to buffet. Similar procedures have been proposed to control higher harmonic vibrations in a helicopter either by oscillating the entire rotor blade or a flap at higher harmonic frequencies. Instead, in the proposed smart structures approach, piezoelectric or other transducers are attached to the airframe and used to apply a control force/moment to the structural system. These actuators and the associated active control can be designed to actively induce an additional damping to the system. In this process, energy of the vibrations of system is transferred to an electronic system from the structural system and thus inducing active damping or electronic damping by the use of airframe mounted actuators.

Such an active structural control system needs sensors, actuator assemblies and controllers. On the basis of the published papers in the field of smart structures, an open research area is the development of methods to provide the needed actuator control authority to reduce vibrations. In reference [6], an offset piezoceramic stack based actuator was introduced. This actuator has the potential to provide the needed control authority to dampen the buffeting-induced vibrations in a rotorcraft. In reference [6], the effectiveness of the offset piezoceramic stack actuator is established through analysis and wind tunnel tests on a 1/16-scaled model of the F-15 aircraft.

In this paper, the subject of the design of the active vibration control of a helicopter is addressed. By the use of piezoceramic stack-based actuators, accelerometer sensors and acceleration feedback controllers, the vibrations due to stabilizer buffeting are to be minimized. Finite element models and available information on the flight loads are used to place the sensors and actuators and design the controller parameters. In a previous paper, feasibility of the use of airframe mounted piezoceramic actuators to control buffet induced vibrations in a rotorcraft was addressed. In this paper, a method is developed to calculate the number of such actuators needed to control the stabilizer buffet induced vibrations.

PROBLEM SETTING

To describe the method of design of the active structural control, we consider a specific rotorcraft that is similar to RAH-66. As can be seen from the flight test data of this rotorcraft[1], there are three frequency bands that are important for buffet induced vibrations. These frequency bands are

- 5 - 8 Hz
- 10 – 13 Hz
- 22 – 25 Hz

An analysis of the flight test data, by the use of the NASTRAN finite element model and load identification procedures, indicates that the bending and torsion modes of the vertical stabilizer are important. The vibration of the vertical stabilizer causes the vibrations of the horizontal stabilizer and the vibration of the fuselage. To obtain a model for the vibration system, we can consider the vertical stabilizer as a beam with coupled bending and torsion vibrations. If we can actively control the bending and torsion vibrations of the vertical tail we can reduce the buffet induced vibrations in the horizontal stabilizer and the fuselage.

Then, the problem is as follows:

1. Can we control the buffet induced vibrations in the rotorcraft by using airframe mounted offset piezoceramic stack actuators, accelerometer sensors and appropriate controllers?

2. How many actuators do we need to control the buffet induced vibrations at all practical forward velocities of the helicopter and at all practical angles of attack? Where should we locate the actuators and sensors?

In this paper, we have developed a method to calculate the number of smart or adaptive actuators assemblies (offset piezoceramic stack actuators) needed to control the buffet-induced vibrations. It has been assumed that the flight test data provide the excitation loads. It has also been assumed that the first bending and first torsion modes of the vertical stabilizer cause primary excitation of the buffet induced vibrations. It is also assumed that the locations of the sensors and actuators can be pre-selected.

To describe the method, the problem is further simplified by using a bending-torsion coupled cantilever beam to model the vertical stabilizer, and use a lumped mass and a lumped inertia to model the

horizontal stabilizer. The dimensions of the ensemble of the empennage are shown in Figure 1.

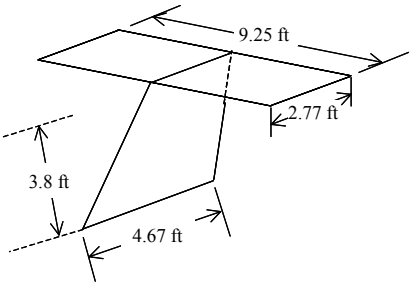

Figure 1 The dimensions of the ensemble of stabilizers

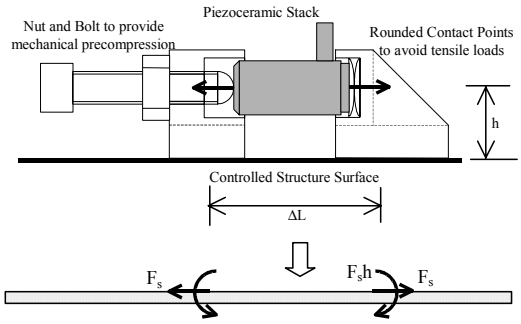

Figure 2 Offset Piezoceramic Stack Actuator Structural Assembly

Based on the previous experience with F-15 stabilizer buffet induced vibration control and the associated successful wind tunnel tests[6], acceleration feedback controller (AFC) is selected. To complete the study, it is necessary to follow these steps.

- As a first step, we have to develop a closed loop model of the vertical stabilizer structural dynamic system, accelerometer sensor, OPSA actuators and AFC (controllers). The effect of the horizontal stabilizer can be considered as a combination of a non-structural mass and lumped inertia. Alternately, we can adjust the frequency of the vertical stabilizer on the basis of the experimental results of the system that consists of both the vertical stabilizer and the horizontal stabilizer. This will be sufficient for considering the first torsional mode response of the vertical stabilizer.

- Then, use the closed loop model to design controller parameters.

- From the controller parameters and the information on exciting loads at 100 knots, the needed maximum control force can be obtained.

- The maximum control force is then used to select the type of the piezoceramic stacks, number of stacks and the associated OPSA design parameters.

This procedure and results are discussed in the following sections.

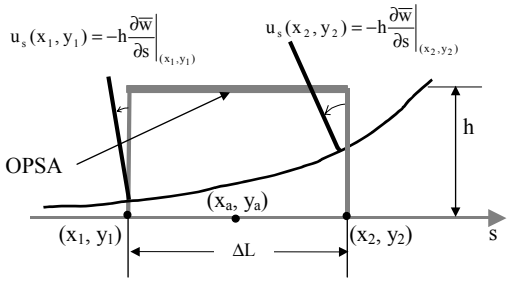

Figure 3 The axial strain of OPSA generated by plate deflection (before and after deformation)

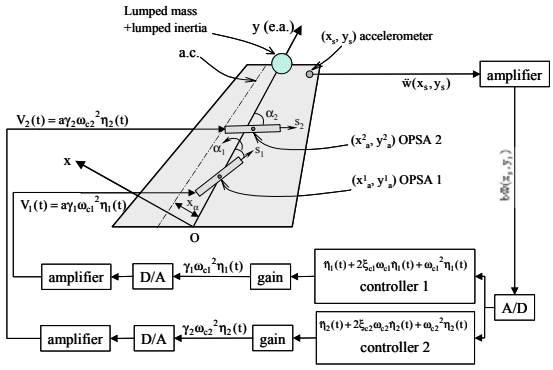

Figure 4 The diagram of the closed-loop active control system

3. Model for the Offset PZT Stack Actuator

An offset PZT stack actuator (OPSA) assembly is shown in Figure 2. It was designed by Bayon de Noyer and Hanagud[6] to transform the longitudinal motion of the stack into moments that will produce the control actuation. OPSA has been successfully applied to F-15 buffeting control. The major advantages of OPSA in comparison to other PZT actuators such as PZT wafers are its large control authority, reliability and maintainability properties. A unidirectional PZT stack that is mounted, as shown in Figure 3, generates a longitudinal (axial) stress. The expression for this stress is given by,

$$\sigma = Y^E{}_s\varepsilon - d_{33}Y^E{}_sE \qquad (1)$$

where ε is the longitudinal strain, σ is the longitudinal stress, Y^E_s is the longitudinal short-circuit Young's modulus, d_{33} is longitudinal piezoelectric constant, and E is the applied electric field. The stabilizer structure is assumed to be in x-y plane and its deflection is given by $\overline{w}(x, y, t)$. The OPSA is placed in the direction of $\vec{s}$ and its center is located at (x_a, y_a). If we assume that the axial strain is uniformly distributed along the span of the piezoceramic stack, the axial strain can be approximated as (as shown in Figure 2 and 3),

$$\varepsilon = \frac{u_s(x_2, y_2) - u_s(x_1, y_1)}{\Delta L} = -\frac{h}{\Delta L}\frac{\partial \overline{w}}{\partial s}\bigg|_{(x_1, y_1)}^{(x_2, y_2)} \tag{2}$$

If we assume that the spontaneous electric field is negligible, i.e. the internal electric field of the piezoceramic stack (PZT) is equal to the acting voltage over the thickness of each layer of PZT stack, and also that the electric field is uniform through the span, the axial force can be approximated by

$$F_s = -k_s^E V(t) - k_s^\varepsilon h\left(\frac{\partial \overline{w}}{\partial s}\bigg|_{(x_1, y_1)}^{(x_2, y_2)}\right) \tag{3}$$

$$\text{where} \quad k_s^\varepsilon = \frac{A_s Y_s^E}{\Delta L};\ k_s^E = \frac{A_s d_{33} Y_s^E}{t_{layer}} \tag{4}$$

and A_s is the cross-section area of PZT. (x_1,y_1) and (x_2,y_2) are the two ends of the PZT supports. V(t) is the voltage and t_{layer} is the thickness of each layer of PZT stack. PZT stack consists of n_{layer} layers of ceramic, i.e. $\Delta L = n_{layer} \times t_{layer}$.

4. Modeling of Closed-Loop System

In this paper, single-input-multiple-output (SIMO) controllers are used. The active control system is presented in Figure 4. The accelerometer is used as a sensor, while multiple OPSAs are assumed to be attached to the stabilizer structure as actuators. The sensor is at (x_s, y_s), the center of the two sets of actuators are located at (x^i_a, y^i_a) (i=1,2) with orientations α_i to the elastic axis. The offset and the length of these OPSAs are h and ΔL, respectively (Figure 2). The forces that the PZT exerts on the stabilizer can be divided into three parts: two point bending moments, two point torsional moments, and an extensional force. All these forces are caused by the longitudinal force of PZT stack. The implemented electric field and the strain caused by the deflection of the stabilizer structure contribute to the longitudinal force of PZT stack. If one actuator does not have enough control authority, more PZT stacks are needed, either at the same or at different positions. However, the outputs of all these PZT stacks are assumed to be additive at approximately the same location. The governing equations for this closed-loop system are given by,

$$\begin{cases} m\dfrac{\partial^2 w}{\partial t^2} - mx_\alpha \dfrac{\partial^2 \theta}{\partial t^2} + \dfrac{\partial^2}{\partial y^2}\left(EI\dfrac{\partial^2 w}{\partial y^2}\right) \\ = -\displaystyle\sum_{i=1}^{n}\left\{ n_s^i F_s^i h \cos\alpha_i \frac{d}{dy}\left[\delta\left(y - y_2^i\right) - \delta\left(y - y_1^i\right)\right]\right\} \\ \quad + f_1(y,t) + f_{h1}\delta(y - L) \\ -I_\alpha \dfrac{\partial^2 \theta}{\partial t^2} + mx_\alpha \dfrac{\partial^2 w}{\partial t^2} + \dfrac{\partial}{\partial y}\left(GJ\dfrac{\partial \theta}{\partial y}\right) \\ = \displaystyle\sum_{i=1}^{2}\left\{ n_s^i F_s^i h \sin\alpha_i \left[\delta\left(y - y_2^i\right) - \delta\left(y - y_1^i\right)\right]\right\} \\ \quad + f_2(y,t) + f_{h2}\delta(y - L) \\ \ddot{\eta}_1(t) + 2\xi_{c1}\omega_{c1}\dot{\eta}_1(t) + \omega_{c1}{}^2\eta_1(t) = b\ddot{\overline{w}}(x_s, y_s, t) \\ \ddot{\eta}_2(t) + 2\xi_{c2}\omega_{c2}\dot{\eta}_2(t) + \omega_{c2}{}^2\eta_2(t) = b\ddot{\overline{w}}(x_s, y_s, t) \end{cases} \tag{5}$$

$$\text{where} \quad f_1(y,t) = \int_c \Delta p(x,y,t)dx; \quad f_2(y,t) = \int_c x\Delta p(x,y,t)dx \tag{6}$$

where m, EI, and GJ are the distributions of mass, bending stiffness, and torsional stiffness. x_α denotes the distance between the elastic axis (e.a.) and center of gravity (c.g.) axis. w(x,t) and θ(y,t) are flexural deflection and the cross-section rotation of the beam. Δp(x,y,t) is the differential pressure distribution of the inboard and outboard of the vertical stabilizer. f_1(y,t) *[lbs×inch^{-1}]* is the generalized aerodynamic bending loads, and f_2(y,t) *[lbs]* is the generalized aerodynamic torsion loads. $\eta_i(t)$ *[volt]* (i=1 and 2) is the control signal. ξ_{ci} and ω_{ci} are controller parameters to be designed. b *[volt×g^{-1}]* is the influence parameters of the sensor. F_s^i is the longitudinal force of the i^{th} set of OPSA stacks. n_s^i is the number of the i^{th} set OPSA stacks. f_{h1} *[lbs]* and f_{h2} *[lbs× inch]* are the equivalent forces of the horzontal stabilizer acting on the vertical stabilizer. The effects of the axial force induced by OPSA on the vertical stabilizer are not included in this model. These terms are of higher order and result in nonlinear equations. The study by

Hanagud *et al* showed the induced frequency changes are small due to these axial force effects[21].

The flexural displacement at any position (x, y) of the stabilizer is given by $\overline{w}(x, y, t)$. That is,

$$\overline{w}(x, y, t) = w(y, t) + x\,\theta(y, t) \tag{7}$$

and axial loads $F_s^{\,i}$ in the i^{th} stack is given by

$$F_s = -k_s^E V_i(t) - k_s^{\varepsilon} h \left(\frac{\partial \overline{w}}{\partial s_i}\bigg|_{(x_1^i, y_1^i)}^{(x_2^i, y_2^i)} \right) \tag{8}$$

where s_i, (x_1^i, y_1^i) and (x_2^i, y_2^i) are the actuator direction, and the two end locations of the i^{th} set of OPSA, respectively. $V_i(t)$ *[volt]* is the control signal voltage, which is the product of the actuator influence parameter a *[1]*, the gain γ_i of the controller and control signals $\omega_{ci}{}^2\eta_i(t)$ (i=1,2). That is,

$$V_i(t) = a\,\gamma_i\,\omega_{ci}{}^2\eta_i(t) \qquad i = 1, \text{and } 2 \tag{9}$$

The following geometric relations are needed for further analysis.

$$\begin{aligned}
&x_1^i = x_a^i - \Delta L \sin\alpha_i / 2; \quad x_2^i = x_a^i + \Delta L \sin\alpha_i / 2;\\
&y_1^i = y_a^i - \Delta L \cos\alpha_i / 2; \quad y_2^i = y_a^i + \Delta L \cos\alpha_i / 2;\\
&\frac{\partial \overline{w}}{\partial s_i} = \frac{\partial \overline{w}}{\partial x}\frac{\partial x}{\partial s_i} + \frac{\partial \overline{w}}{\partial y}\frac{\partial y}{\partial s_i} = \frac{\partial \overline{w}}{\partial x}\sin\alpha_i + \frac{\partial \overline{w}}{\partial y}\cos\alpha_i;\\
&\qquad\qquad\qquad\qquad\qquad\qquad\qquad\qquad\qquad\qquad i = 1, \text{and } 2
\end{aligned} \tag{10}$$

We employ Galerkin's method and include two important comparison functions of the stabilizer structure.

$$\overline{w}(x, y, t) = \sum_{i=1}^{2} g_i(x, y) q_i(t) \tag{11}$$

Where $g_i(x,y)$ is the approximate i^{th} coupled flexural-torsional mode shape. If we assume that the changes of the mode shapes due to the lumped mass and inertia are negligible, then

$$g_i(x, y) = \left[A_i f(y) + x\,B_i \phi(y) \right] \tag{12}$$

Where f(y) and ϕ(y) are the 1st pure bending and torsion mode of cantilever beam/rod. A_i and B_i are non-dimensional constants. Then,

$$\begin{aligned}
&w(y, t) = f(y)\left[A_1 q_1(t) + A_2 q_2(t)\right];\\
&\theta(y, t) = \phi(y)\left[B_1 q_1(t) + B_2 q_2(t)\right]
\end{aligned} \tag{13}$$

Substituting equation (13) into equation (10e),

$$\begin{aligned}
\frac{\partial \overline{w}}{\partial s_i} = &\left(B_1\phi(y)\sin\alpha_i + \left(A_1 \frac{df}{dy} + B_1 x \frac{d\phi}{dy} \right)\cos\alpha_i \right) q_1(t)\\
&+ \left(B_2\phi(y)\sin\alpha_i + \left(A_2 \frac{df}{dy} + B_2 x \frac{d\phi}{dy} \right)\cos\alpha_i \right) q_2(t)
\end{aligned} \tag{14}$$

Substituting equation (14) into (5), multipying equation (5a) and (5b) by f(y) and ϕ(y) respectively, and integrating with respect to y from 0 to L (Galerkin's method), we can obtain,

$$\begin{cases}
\left(c_{11}A_1 - c_{12}B_1\right)\ddot{q}_1 + \left(c_{11}A_2 - c_{12}B_2\right)\ddot{q}_2 + a_{11}\left(A_1 q_1 + A_2 q_2\right)\\
\quad = \sum_{i=1}^{2} n_s^i F_s^i h \cos\alpha_i \left(\frac{df}{dy}\Big|_{y=y_1^i}^{y=y_2^i} \right) + \int_0^L f_1(y,t) f(y)\,dy + f_{h1} f(L)\\
\left(c_{21}A_1 - c_{22}B_1\right)\ddot{q}_1 + \left(c_{21}A_2 - c_{22}B_2\right)\ddot{q}_2 - a_{22}\left(B_1 q_1 + B_2 q_2\right)\\
\quad = \sum_{i=1}^{2} n_s^i F_s^i h \sin\alpha_i \left(\phi(y)\big|_{y=y_1^i}^{y=y_2^i} \right) + \int_0^L f_2(y,t)\phi(y)\,dy + f_{h2}\phi(L)\\
\ddot{\eta}_1(t) + 2\xi_{c1}\omega_{c1}\dot{\eta}_1(t) + \omega_{c1}{}^2\eta_1(t)\\
\quad = b\left\{ f(y_s)\left(A_1\ddot{q}_1 + A_2\ddot{q}_2\right) + x_s\phi(y_s)\left(B_1\ddot{q}_1 + B_2\ddot{q}_2\right) \right\}\\
\ddot{\eta}_2(t) + 2\xi_{c2}\omega_{c2}\dot{\eta}_2(t) + \omega_{c2}{}^2\eta_2(t)\\
\quad = b\left\{ f(y_s)\left(A_1\ddot{q}_1 + A_2\ddot{q}_2\right) + x_s\phi(y_s)\left(B_1\ddot{q}_1 + B_2\ddot{q}_2\right) \right\}
\end{cases} \tag{15}$$

Where

$$a_{11} = \int_0^L \left(\frac{d^2}{dy^2}\left[EI \frac{d^2 f}{dy^2} \right] \right) f\,dy;$$

$$a_{22} = -\int_0^L \left(\frac{d}{dy}\left[GJ \frac{d\phi}{dy} \right] \right) \phi\,dy \;[\text{lbs}\cdot\text{in}]$$

$$c_{11} = \int_0^L m f^2 dy; \quad c_{22} = \int_0^L \left(I_\alpha \phi^2 \right) dy \;[\text{slugs}\cdot\text{in}^2];$$

$$c_{12} = c_{21} = \int_0^L \left(m x_\alpha \phi f \right) dy \;[\text{slugs}\cdot\text{in}^2]$$

To increase the control force and to achieve the maximum control authority, OPSA set 1 that is used to control the 1st bending mode is placed along the elastic axis, i.e. α_1=0°; while OPSA set 2 that are employed to control the 1st torsion mode is placed at a orientation of α_2 to elastic axis, e.g. α_2=45°. For the first two modes, the torsion-bending couplings are negligible. The torsion-bending coupling caused by

the performance the PZT stacks are also neglected because these effects are small. Then, equation (15) becomes,

$$\begin{cases} \ddot{q}_1 + \omega_1^2 q_1 = -n_s^1 \bar{a}_{11}\gamma_1\omega_{c1}^2\eta_1 - n_s^2\bar{a}_{12}\gamma_2\omega_{c2}^2\eta_2 + \bar{f}_1(t) \\ \ddot{q}_2 + \omega_2^2 q_2 = -n_s^1 \bar{a}_{21}\gamma_1\omega_{c1}^2\eta_1 - n_s^2\bar{a}_{22}\gamma_2\omega_{c2}^2\eta_2 + \bar{f}_2(t) \\ \ddot{\eta}_1(t) + 2\xi_{c1}\omega_{c1}\dot{\eta}_1(t) + \omega_{c1}^2\eta_1(t) = b\{f(y_s)\ddot{q}_1 + x_s\phi(y_s)\ddot{q}_2\} \\ \ddot{\eta}_2(t) + 2\xi_{c2}\omega_{c2}\dot{\eta}_2(t) + \omega_{c2}^2\eta_2(t) = b\{f(y_s)\ddot{q}_1 + x_s\phi(y_s)\ddot{q}_2\} \end{cases} \tag{16}$$

Where

$$\bar{f}_1(t) = \frac{f_1(t)}{c_{11}};\quad \bar{f}_2(t) = \frac{f_2(t)}{c_{22}};\quad \bar{a}_{1i} = \frac{a_{1i}}{c_{11}};\quad \bar{a}_{2i} = \frac{a_{2i}}{c_{22}};$$

$$f_1(t) = \int_0^L f_1(y,t)f(y)dy + f_{h1}f(L);$$

$$f_2(t) = \int_0^L f_2(y,t)\phi(y)dy + f_{h2}\phi(L);\ [\text{lbs}\times\text{in}]$$

$$a_{1i} = a\,h\cos\alpha_i k_s^E\left(\left.\frac{df}{dy}\right|_{y=y_1^i}^{y=y_2^i}\right);$$

$$a_{2i} = a\,h\sin\alpha_i k_s^E\left[\phi(y_2^i) - \phi(y_1^i)\right];\ [\text{lbs}\cdot\text{in}\cdot\text{volt}^{-1}]$$

$$\bar{\omega}_1^2 = \omega_1^2 + \frac{ah^2\cos\alpha_1}{c_{11}}n_s^1 k_s^\varepsilon\left(\left.\frac{df}{dy}\right|_{y=y_1^1}^{y=y_2^1}\right)^2; \tag{17}$$

$$\bar{\omega}_2^2 = \omega_2^2 + \frac{ah^2\sin\alpha_2}{c_{22}}n_s^2 k_s^\varepsilon\left[\phi(y_2^2) - \phi(y_1^2)\right]^2$$

$$i = 1, \text{and } 2$$

where $\bar{a}_1$ and $\bar{a}_2$ are the generalized modal influence parameters of the actuator for the 1st and 2nd modes. $\bar{f}_1(t)$ and $\bar{f}_2(t)$ are the generalized modal loads. Since the actuator will stiffen the structure, it is seen from equation (17i) and (17j) that the stacks increase the natural frequencies ω_1 and ω_2. The frequencies increase with the offset h, the axial stiffness of the stacks, number of the stacks and curvature of the structure at the actuator locations.

In further numerical illustration, the problem is simplified by considering only the torsion mode of the vertical stabilizer. This induces a yaw-motion in the horizontal stabilizer structure. Then, γ_1=0, i.e. OPSA set 1 is removed. Then, the system is uncoupled into two sets of one-degree system except that the sensor signal is coupled. It is noted that it is practicly impossible to separate pure torsion response from the sensor signal. However, we only consider the frequency band around 11.6 Hz, at which the bending response is smaller than the torsion response. Then, we obtain signal around 11.6 Hz for controlling the system. Then,

$$\begin{cases} \ddot{q}_2 + 2\xi_2\omega_2 q_2 + \omega_2^2 q_2 = -n_s^1\,\bar{a}_{22}\gamma_2\omega_{c2}^2\eta_2(t) + \bar{f}_2(t) \\ \ddot{\eta}_2(t) + 2\xi_{c2}\omega_{c2}\dot{\eta}_2(t) + \omega_{c2}^2\eta_2(t) \approx \bar{b}\ddot{q}_2 \end{cases} \tag{18}$$

Where $\bar{b} = bx_s\phi(y_s)$ *[volt×inch×g^{-1}]* is the total influence parameter of sensor. The modal damping that can be obtained from experimental measurement is added to the system as in equation (18). The modal frequency is adjusted according to the experiments (so the effects of horizontal stabilizer on the modes are accounted). The system described in equation (18) is a single degree of freedom structural system with acceleration feedback control. The crossover point theory[6] is used to design control parameters.

5. Single Degree of Freedom Acceleration Feedback Control

According to equation (18), we can get the transfer functions of both the open- and the closed- loop systems. The transfer function of the response and excitation for the open-loop system is given by equation (19). Equation (20), (21) and (22) give the transfer functions of the excitation and the response, the controller signal and response, the controller signal and the excitation for the closed-loop system, respectively.

$$G_{qf}^{op}(s) = \frac{Q_2^{op}(s)}{\bar{F}_2(s)} = \frac{1}{(s^2 + 2\xi_2\omega_2 s + \omega_2^2)} \tag{19}$$

$$G_{qf}^{cl}(s) = \frac{Q_2^{cl}(s)}{\bar{F}_2(s)} = \frac{(s^2 + 2\xi_{c2}\omega_{c2}s + \omega_{c2}^2)}{(s^2 + 2\xi_2\omega_2 s + \omega_2^2)(s^2 + 2\xi_{c2}\omega_{c2}s + \omega_{c2}^2) + \gamma_2\omega_{c2}^2 n_s^2\bar{a}_{22}\bar{b}s^2} \tag{20}$$

$$G_{\eta q}^{cl}(s) = \frac{I_2(s)}{Q_2^{cl}(s)} = \frac{\bar{b}s^2}{(s^2 + 2\xi_{c2}\omega_{c2}s + \omega_{c2}^2)} \tag{21}$$

$$G_{\eta f}^{cl}(s) = \frac{I_2(s)}{\bar{F}_2(s)} = \frac{\bar{b}s^2}{(s^2 + 2\xi_2\omega_2 s + \omega_2^2)(s^2 + 2\xi_{c2}\omega_{c2}s + \omega_{c2}^2) + \gamma_2\omega_{c2}^2 n_s^2\bar{a}_{22}\bar{b}s^2} \tag{22}$$

The Laplace transform of each variable is represented by the corresponding capital letter. $I_2(s)$ is the Laplace transform of $\eta_2(t)$. The subscripts 'op' and

'cl' represent 'open-loop' and 'close-loop'. The crossover point, i.e. a single closed-loop natural frequency resulting for the 2 degree of freedom system equation (18), is obtained when the roots of the closed-loop characteristic equation, i.e. the denominator of equation (20), are repeated complex conjugate pairs. This yields,

$$(s^2 + 2\xi_2\omega_2 s + \omega_2{}^2)(s^2 + 2\xi_{c2}\omega_{c2}s + \omega_{c2}{}^2) + \gamma_2\omega_{c2}{}^2 n_s{}^2\bar{a}_{22}\bar{b}s^2 = (s^2 + 2\xi_f\omega_f s + \omega_f{}^2)^2 \quad (23)$$

Where ω_f and ξ_f are the natural frequency and damping ratio of the closed-loop system, respectively. We have five unknowns as $\xi_{c2}, \omega_{c2}, \gamma_2, \omega_f, \xi_f$. Equating the coefficients the power of s,

$$\begin{cases} \xi_2\omega_2 + \xi_{c2}\omega_{c2} = 2\xi_f\omega_f \\ \omega_2{}^2 + \omega_{c2}{}^2 + 4\xi_{c2}\omega_{c2}\xi_2\omega_2 + \gamma_2\omega_{c2}{}^2 n_s{}^2\bar{a}_{22}\bar{b} = 2\omega_f{}^2 + 4\xi_f{}^2\omega_f{}^2 \\ \xi_{c2}\omega_2 + \xi_2\omega_{c2} = 2\xi_f\omega_f \\ \omega_2\omega_{c2} = \omega_f{}^2 \end{cases} \quad (24)$$

A practical choice of parameters to satisfy equation (24) is

$$\omega_{c2} = \omega_f = \omega_2;\ \xi_f = \frac{\xi_{c2} + \xi_2}{2};\ \gamma_2 = \frac{(\xi_{c2} - \xi_2)}{n_s{}^2\bar{a}_{22}\bar{b}} \quad (25a\text{-}c)$$

The controller and the closed-loop system have the same frequency as the open-loop system ω_2. Since the damping of open loop system is usually quite small about 0.1-0.2%[1][13-14], we can significantly increase the damping of the closed-loop system by selecting or designing a large controller damping. The desired controller gain is proportional to the selected controller damping, and can be reduced by adjusting the influence parameters of the actuator and sensor $\bar{a}_{22}$ and $\bar{b}$, or by increasing the number of the stacks. It is noted from equation (17c,g) that, increasing OPSA offset, and/or selecting high performance piezoceramic stack, and/or placing OPSA at the position of large curvature can increase the actuator influence parameters.

From equations (19-20) and (23),

$$\left|\frac{Q_2^{cl}(j\omega)}{Q_2^{op}(j\omega)}\right|^2 = \left|\frac{\left(4\xi_2{}^2\omega_2{}^2\omega^2 + (\omega_2{}^2 - \omega^2)^2\right)\left(4\xi_{c2}{}^2\omega_{c2}{}^2\omega^2 + (\omega_2{}^2 - \omega^2)^2\right)}{\left(4\xi_f{}^2\omega_2{}^2\omega^2 + (\omega_2{}^2 - \omega^2)^2\right)^2}\right|^2$$

When $\xi_{c2} >> \xi_2$, the closed-loop response is reduced significantly in comparison to open-loop response at $\omega=\omega_1$. For example, if $\xi_{c2} = 10\xi_2$, then

$$\left[\left|\frac{\omega^2 Q_2^{cl}(j\omega)}{\omega^2 Q_2^{op}(j\omega)}\right|^2\right]_{\omega=\omega_2} = \left(\frac{4\xi_2/\xi_{c2}}{(1+\xi_2/\xi_{c2})^2}\right)^2 = \left(\frac{0.4}{1.4^2}\right)^2 = 4.2\%$$

6. Controller Authority Analysis and Minimum Number of Needed Actuators

From equations (21) and (22),

$$I_2(j\omega) = \frac{-\bar{b}\omega^2}{(j2\xi_f\omega_f\omega + \omega_f{}^2 - \omega^2)^2}\bar{F}_2(j\omega) \quad (28)$$

As noted before, $I_2(j\omega)$ is the frequency response of $\eta_2(t)$. To calculate the authority of the controller, we consider the worst situation, that is, $\omega = \omega_2 (= \omega_f = \omega_{c2})$,

$$\left|I_2\right|_{\omega=\omega_2} = \frac{\bar{b}}{(\xi_{c2} + \xi_2)^2\omega_2{}^2}\left|\bar{F}_2(j\omega)\right|_{\omega=\omega_2} \quad (29)$$

From equations (8) and (9), we obtain the expression for the blocked force as $|F_c|$ as,

$$|F_c| = k_s^E |V_2| = k_s^E a\gamma_2\omega_{c2}{}^2 |I_2| \quad (30)$$

Which, at any situation including $\omega = \omega_2$, cannot be greater than the maximum blocked force $|F_c|_{max}$ (manufacturer's listed value). That means,

$$|F_c|_{\omega=\omega_2} = k_s^E a\gamma_2\omega_{c2}{}^2 |I_2|_{\omega=\omega_2} \le |F_c|_{max} \quad (31)$$

Therefore, we can obtain that

$$\gamma_2 \le \frac{|F_c|_{max}}{k_s^E a\omega_{c2}{}^2 |I_2|_{\omega=\omega_2}} \quad (32)$$

Substituting equation (29) into (32) and rearranging terms, the maximum gain under the expected operation is given by,

$$\gamma_{2,max} = \frac{|F_c|_{max}}{k_s^E a\,\omega_{c2}{}^2 |I_2|_{max}} = \frac{(\xi_{c2} + \xi_2)^2}{a\bar{b}k_s^E}\frac{|F_c|_{max}}{\left|\bar{F}_2(j\omega_2)\right|} \quad (33)$$

(27)

To guarantee that the controller gain can achieve the performance requirements and warrant the

operational safety of the stack, the designed gain from equation (25c) should be always not greater than the maximum gain given in equation (33). This means,

$$\gamma_{2,\text{design}} \le \gamma_{2,\max} \Leftrightarrow \frac{(\xi_{c2}-\xi_2)}{n_s^2 \bar{a}_{22} \bar{b}} \le \frac{(\xi_{c2}+\xi_2)^2}{a\,\bar{b} k_s^E} \frac{|F_c|_{\max}}{\left|\bar{F}_2(j\omega_2)\right|} \tag{34}$$

From equation (34) and equations (16b,d, and h), we obtain that the minimum number of needed stacks $n^2_{s,\min}$ is given by

$$n^2_{s,\min} = \frac{(\xi_{c2}-\xi_2)}{(\xi_{c2}+\xi_2)^2} \frac{a k_s^E \left|\bar{F}_2(j\omega_2)\right|}{\bar{a}_{22} |F_c|_{\max}}$$
$$= \frac{(\xi_f-\xi_2)}{2\xi_f^{\,2}} \frac{1}{h\Delta L \sin\alpha_2} \left[\frac{\phi(y_2^2)-\phi(y_1^2)}{\Delta L}\right]^{-1} \frac{\left|\bar{F}_2(j\omega_2)\right|}{|F_c|_{\max}} \tag{35}$$

Usually, the designed damping ratio ξ_f for closed-loop system is much larger than damping ratio ξ_2 of the open-loop system. Then,

$$n_{s,\min} \approx \frac{1}{\xi_f\, h\Delta L \phi'(y_a^2)\sin(2\alpha_2)} \frac{\left|\bar{F}_2\right|_{\max}}{|F_c|_{\max}} \tag{36}$$

It is seen that the minimum number of needed stacks is proportional to the magnitude of the maximum encountered aerodynamic loads. However, the number can be reduced through the choice of high performance PZT stacks (large blocked force), and/or placing the stacks with large slope α_2 to elastic axis and/or at the position with steep torsion deformation, and/or increasing the offsets.

From the flight test data at 100 knots, PSD of differential pressure at frequency 11.6 Hz at a typical location (7% chord 30% span) on the vertical stabilizer is adapted from Figure 4.35 of Ref [1]. From PSD of this typical point, we can calculate PSD of the generalized aerodynamic modal load according to Equation (A5) in Appendix. However, only the 2nd generalized aerodynamic modal load is needed. It is,

$$\mathbf{PSD}\big|_{f=11.6hz} = 0.75\times10^{-3}\ \text{psi}^2;\quad f_{h2} \approx 0 \tag{37}$$

$$\text{PSD}_2\big|_{f=11.6hz} = \mathbf{PSD}\big|_{f=11.6hz} \left(\iint_A x\phi(y)\,dx\,dy\right)^2$$
$$= 2.67\times10^5\ \text{psi}^2\text{in}^6 \tag{38}$$

Then,

$$|\bar{F}_2|_{f=11.6hz} = 5.16\times10^2\ \text{lbs}\cdot\text{in} \tag{39}$$

Fixing two parameters, i.e. ΔL = 5.7 in (real dimension used in F15 lab at Gatech) and the closed-loop damping ratio ξ to be 0.5, OPSA is placed at the location close to the root (with largest torsion moment) and α_2=45°. The number of stacks needed for different performance PZT stack and OPSA offset is calculated and listed in Table 1.

Table 1 Number of PZT Stacks

	Offset h		
	1 inch	2.5 inch	4 inch
P-830.10 (1kN)	17	7	5
P-247.70 (48kN)	1	1	1

Table 2. Open Loop Parameters
(Determined by horizontal Stabilizer Data[1])

	Frequency	Damping Ratio
Horiz Stab Yaw Mode	11.8	0.8%

Table 3. Designed Controllers for Yaw Mode

	Controller		
	Freq1	Damping Ratio1	Gain1
Design 1	11.8	3.5%	0.12
Design 2	11.8	9.5%	1.12

7. Controller Parameters and Performance

The open-loop modal information obtained from reference [1] is presented in Table 2. The damping ratios are obtained from experimental measurement. And the desgined controllers are shown in Table 3, and shown in Figure 5 that is obtained from following the precedure dissussed above.

In Table 3, the placement of OPSA is the same as shown before. PI P-247.70 HVPZT (48kN) is used as the actuator, and PCB 303A02 accelerometer is used (b=10mv/g). The stack number is chosen to be 1 and

h=2.5in. The actuator influence parameter is 10 (a=10).

To estimate the reduction of AFC, the reductions of PSD of longitudinal response at horizontal stabilizer left tip at 100 knots are calculated and presented in Figure 6. The reductions for design 1 and 2 at the peak are 70% and 90%, respectively. The open loop data is obtained from ref [1].

Figure 5 Transfer Functions of Controllers

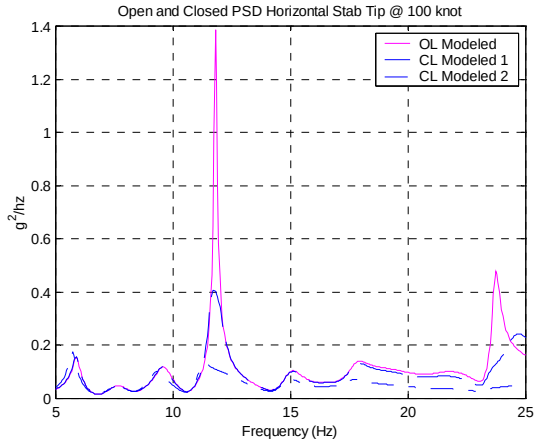

Figure 6 Comparison of the Frequency Response with and without Controllers

CONCLUSIONS

It has been shown that acceleration feed back controllers can be designed with smart structures-based offset piezoceramic stack actuators (OPSA) to control buffet-induced vibrations. The OPSA actuators have the potential to provide sufficient control authority to control the vibrations. To accurately design minimum weight controllers with sufficient control authority, questions of optimum placement of these actuators and optimum design of the controllers must be addressed. Observability issues should also be addressed where necessary. The resulting controllers should be validated in wind tunnel tests and flight tests.

APPENDIX

Generalized Aerodynamic Modal Loads

If the distribution of differential pressure $\Delta p(x,y,t)$ is measured, the generalized aerodynamic modal loads for the i^{th} mode can be obtained as

$$Q_i(t) = \iint_A \Delta p(x,y,t) g_i(x,y) dx dy \qquad i = 1,2,\cdots \qquad (A1)$$

The auto-correlation of the i^{th} modal load is calculated as

$$R_{ii}(t) = \int_{-\infty}^{t} Q_i(t-\tau) Q_i(\tau) d\tau \qquad i = 1,2,\cdots \qquad (A2)$$

If we assume spatial 100% correlation, that means the correlation between any two locations (x,y) and (ξ,η) is the same, i.e.,

$$\boldsymbol{R}_{(x,y)(\xi,\eta)}(t) = \int_{-\infty}^{t} \Delta p(x,y,t-\tau) \Delta p(\xi,\eta,\tau) d\tau = \boldsymbol{R}(t) \qquad (A3)$$

It is noted that the notations for the modal correlation and position correlation are distinguished by normal and bold "R". PSD of position correlation is denoted by bold letters **PSD**, which is made different from normal letters PSD for modal correlation. Therefore, the correlation of the i^{th} modal load can be obtained by

$$\begin{aligned} R_{ii}(t) &= \int_{-\infty}^{t} \left(\iint_A \Delta p(x,y,t-\tau) g_i(x,y) dx dy \right) \left(\iint_A \Delta p(\xi,\eta,\tau) g_i(\xi,\eta) d\xi d\eta \right) d\tau \\ &= \iint_A \iint_A \left(\int_{-\infty}^{t} \Delta p(x,y,t-\tau) \Delta p(\xi,\eta,\tau) d\tau \right) g_i(\xi,\eta) g_i(x,y) d\xi d\eta dx dy \\ &= \iint_A \iint_A \boldsymbol{R}(t) g_i(\xi,\eta) g_i(x,y) d\xi d\eta dx dy \\ &= \boldsymbol{R}(t) \left(\iint_A g_i(\xi,\eta) d\xi d\eta \right)^2 \end{aligned} \qquad (A4)$$

Then, the PSD of the i^{th} modal load can be obtained by

$$PSD_i(\omega) = \int_{-\infty}^{\infty} R_{ii}(t)e^{-j\omega t}dt = \mathbf{PSD}(\omega)\left(\iint_A g_i(\xi,\zeta)d\xi d\zeta\right)^2 \quad \text{(A5)}$$

REFERENCES

[1] Mason, P.H., Identification of Random Loads Impinging on RAH-66, M.S. Thesis, Naval Postgraduate School, approved for public release; distribution is unlimited, 1998

[2] Nitzsche, F; Zimcik, DG; Ryall, TG; Moses, RW; Henderson, DA, "*Control law synthesis for vertical fin buffeting alleviation using strain actuation*", 40th AIAA/ASME/ASCE/AHS/ASC Structures, Structural Dynamics, and Materials Conference, 1999, AIAA-99-1317.

[3] Moses, R.W., "*Vertical-stabilizer-buffeting alleviation using piezoelectric actuators: some results of the actively controlled response of buffet-affected stabilizers (ACROBAT) program*", Proc. SPIE, v. 3044, 1997, pp. 87-98.

[4] Moses, R.W., "*Contributions to active buffeting alleviation programs by the NASA Langley Research Center*", 40th AIAA/ASME/ASCE/AHS/ASC Structures, Structural Dynamics, and Materials Conference, 1999, AIAA-99-1318.

[5] Pado, L. E., and Lichtenwalner, P. F., "*Neural predictive control for active buffet alleviation*", 40th AIAA/ASME/ASCE/AHS/ASC Structures, Structural Dynamics, and Materials Conference, v. 2, 1999, pp. 1043-1053, (AIAA-99-1319).

[6] Hanagud, S., et. al. " Stabilizer Buffet Alleviation of High Performance Twin Stabilizer Aircraft Using Piezo Stack Actuators", AIAA Paper No. AIAA- 99-1320, Proceedings of AIAA/ASME/ASCE/AHC structures, structural Dynamics and Materials conference, 1999

[7] Nitche, F., et.al., Finite Element Approach for Design Control algorithms for Vertical fin Buffeting using Strain Actuation, Pre-print, NATO Active Control Technology Conference, Braunschweig, Germany, May, 2000

[8] Ashley, H., Rock, S.M., Digumarthi, R., Channey, K. and Eggers, A.J., "*Active Control for Fin Buffet Alleviation*", WL-TR-93-3099, 1994.

[9] Lazarus, K.B., Saarmaa, E., and Agnes, G.S., "*Active smart material system for buffet load alleviation*", Proc. SPIE, v. 2447, 1995, pp. 179-192.

[10] Moore, J.W., Spangler, R.L., Lazarus, K.B. and Henderson, D.A., "*Buffet load alleviation using distributed piezoelectric actuators*", Industrial and Commercial Applications of Smart Structures Technologies, ASME, AD v. 52, 1996, pp. 485-490.

[11] Spangler, R.L., and Jacques, R.N., "*Testing of an active smart material system for buffet load alleviation*", 40th AIAA/ASME/ASCE/AHS/ASC Structures, Structural Dynamics, and Materials Conference, 1999, AIAA-99-1317.

[12] Hauch, R.M., Jacobs, J.H., Ravindra, K., and Dima, C., "*Reduction of vertical stabilizer buffet response using active control*", J. of Aircraft, v. 33, n. 3, 1996, pp. 617-622.

[13] Nitzsche, F. ,Zimcik, D.G., and Langille, K., "*Active control of vertical fin buffeting with aerodynamic control surface and strain actuation*", 38th AIAA/ASME/ASCE/AHS/ASC Structures, Structural Dynamics, and Materials Conference., v. 2, 1997, pp. 1467-1477.

[14] Preumont, A., "*Vibration Control of Active Structures: An Introduction*", Kluwer Academic Publishers, 1997.

[15] Zhou, K., Doyle, C.D., and Glover, K., "*Robust and Optimal Control*", Prentice-Hall, 1996.

[16] Balas, M.J., "*Active Control of Flexible Systems*", J. of Optimization Theory and Applications, Vol. 25, No. 3, 1978, pp. 415-436.

[17] Goh, C. J. and Caughey, T. K., "*On the stability problem caused by finite actuator dynamics in the collocated control of large space structures*", International Journal of Control, Vol. 41, No. 3,1985, pp. 787-802.

[18] Juang, J. N. and Phan, M., "*Robust Controller Designs for Second-Order Dynamic Systems: A Virtual Passive Approach*", Journal of Guidance, Control and Dynamics, Vol. 15, No. 5, 1992, pp. 1192-1198.

[19] Sim, E. and Lee, S. W., "*Active Vibration Control of Flexible Structures with Acceleration Feedback*", Journal of Guidance, Vol. 16, No. 2, 1993, pp. 413-415.

[20] Goh, C. J. and Yan, W. Y., "*Approximate Pole Placement for Acceleration Feedback Control of Flexible Structures*", Journal of Guidance, Vol. 19, No. 1, 1996, pp. 256-259.

[21] Roberts, P. and Hanagud, S, "Model based simulation of the Active damping of a Cantilever Plate and Redistribution of Stresses ", Adaptive Structures and Material Systems, ASME, 2000, in press.

[22] S. Hanagud, X. Lu, P. Roberts, "Model Based Simulation of Buffet-induced vibration control of a f/a-18 vertical stabilizer", AIAA Paper No. AIAA-2001-1352, Proceedings of AIAA/ASME/ASCE/AHC structures, structural Dynamics and Materials conference, 2001